PERGAMON

Available online at www.sciencedirect.com

SCIENCE DIRECT®

Polyhedron 22 (2003) 189–197

POLYHEDRON

www.elsevier.com/locate/poly

Tuneable crystal host properties in (pyridyloxy)cyclotetraphosphazenes

Eric W. Ainscough *, Andrew M. Brodie *, Andreas Derwahl

Chemistry-Institute of Fundamental Sciences, Massey University, Private Bag 11222, Palmerston North, New Zealand

Received 6 August 2002; accepted 11 October 2002

Abstract

The single crystal X-ray structures of octakis(4-methyl-2-pyridyloxy)cyclotetraphosphazene bis(dichloromethane) (**2**) and the monohydrate (**3**), reveal the presence of approximately 7.5 and 5.5 Å diameter tunnels, respectively, which entrap the solvent molecules. In contrast, the non-methyl-substituted parent, octakis(2-pyridyloxy)cyclotetraphosphazene (**1**), does not form an inclusion compound. For compounds **1** and **2**, the cyclotetraphosphazene ring adopts a centrosymmetric chair conformation, whereas in **3**, it has a twisted geometry. The importance of intermolecular and intramolecular interactions in determining these structural differences is discussed.

Keywords: Octakis(2-pyridyloxy)cyclotetraphosphazene; Octakis(4-methyl-2-pyridyloxy)cyclotetraphosphazene; Inclusion compounds; X-ray structures

1. Introduction

The formation of inclusion adducts by the entrapment of small molecules into the lattices of a range of organic host compounds, to form supramolecular assemblies, is receiving considerable attention [1]. Such hosts show potential in many areas, e.g. as templates for polymerisation reactions, for the separation of molecules, for non-linear optical activity, for drug purification and for trapping and storage of toxic materials [2]. The importance of seemingly weak, non-covalent intermolecular interactions, rather than normal covalent bonds, in the formation of inclusion (or clathrate) compounds is well documented [1]. However, the routine design of crystalline guests with specific host-binding properties is still not possible, although likely determining factors may be examined [3]. Most studies have concentrated on hosts that create a fixed cavity for a specific guest, but fewer studies have been performed on a host that may have the cavity or channel dimensions (known as cavity tuning) altered by the guests. In this report, we show that a change in the intermolecular interactions in a pyridyloxy-substituted cyclotetraphosphazene host alters the dimensions of its channels.

To date, reports of clathrates of phosphazenes have focussed exclusively on cyclotriphosphazenes [4–6], and in particular on aromatic dioxy-substituted spirocyclotriphosphazenes. For example, Allcock and Sunderland [6] showed that tris(*o*-phenylenedioxy)cyclotriphosphazene will separate mixtures of small molecules as well as macromolecules by selective clathration. In such compounds the arrangement of the paddle-wheel-shaped cyclotriphosphazenes is dominated by van der Waals interactions of the substituents with the guest molecules, thus forming hexagonal-shaped tunnels of adjustable size. The tunnels can be penetrated by various linear compounds including alkanes, alkanediols or polymers (e.g. polyethylene, polybutadiene, poly(tetramethylene oxide).

Cyclotetraphosphazenes, which contain flexible eight-membered rings rather than the rigid planar six-membered rings seen in their trimer analogues [7], are not able to form paddle-wheel-shaped crystalline hosts. Nevertheless, in this paper we report they can be used to engineer hosts with tubular tunnels provided an

* Corresponding authors. Tel.: +64-6-356-9099; fax: +64-6-356-5682

E-mail addresses: e.ainscough@massey.ac.nz (E.W. Ainscough), a.brodie@massey.ac.nz (A.M. Brodie).

0277-5387/02/$ - see front matter
PII: S0277-5387(02)01332-3

appropriate substituent, which is capable of forming two- and three-dimensional hydrogen-bond networks, is used. It appears that the ability of the cyclophosphazene ring nitrogen atoms to contribute to this network can be fine-tuned by altering the substituents on the phosphorus ring atoms. Hence we describe how the introduction of the 4-methyl substituent into the pyridyloxy rings of octakis(2-pyridyloxy)cyclotetraphosphazene (**1**) causes a change in the crystal structure of the cyclotetraphosphazene to a clathrate-type structure with tunnels extending through the lattice which are occupied by either dichloromethane, (compound **2**) or water (compound **3**) guest molecules.

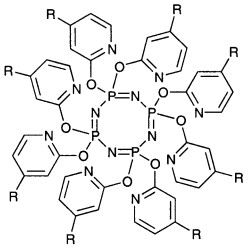

Compound **1**, $N_4P_4(OC_5H_4N)_8$ R = H
Compound **2**, $N_4P_4(OC_6H_6N)_8{\cdot}2CH_2Cl_2$ R = CH_3
Compound **3**, $N_4P_4(OC_6H_6N)_8{\cdot}H_2O$ R = CH_3

2. Results and discussion

2.1. Synthesis of compounds 1, 2 and 3

Octakis(2-pyridyloxy)cyclotetraphosphazene (**1**) was prepared from the reaction of the sodium salt of 2-hydroxypyridine with $N_4P_4Cl_8$ in tetrahydrofuran (THF) and recrystallised from CH_2Cl_2–pentane. Compound **2**, $N_4P_4(OC_6H_6N)_8{\cdot}2CH_2Cl_2$, was similarly prepared but using the sodium salt of 4-methyl-2-hydroxypyridine. The solvated dichloromethane was readily lost and upon recrystallisation of **2** from 1,3-dichloropropane, compound **3**, $N_4P_4(OC_6H_6N)_8{\cdot}H_2O$, was obtained, the occluded water arising from traces of it present in the solvent.

2.2. Structures of compounds 1, 2 and 3

2.2.1. The cyclotetraphosphazene rings

The single crystal X-ray structures of compounds **1** and **2** both show the cyclotetraphosphazene ring adopts a centrosymmetric chair conformation with all four ring nitrogen atoms [N(1), N(2), N(1#) and N(2#)] and two of the phosphorus atoms [P(2) and P(2#)] in a well defined plane leaving the other two phosphorus atoms [P(1) and P(1#)] to lie above and below it (Figs. 1 and 2). This conformation is also the most stable form (T-form)

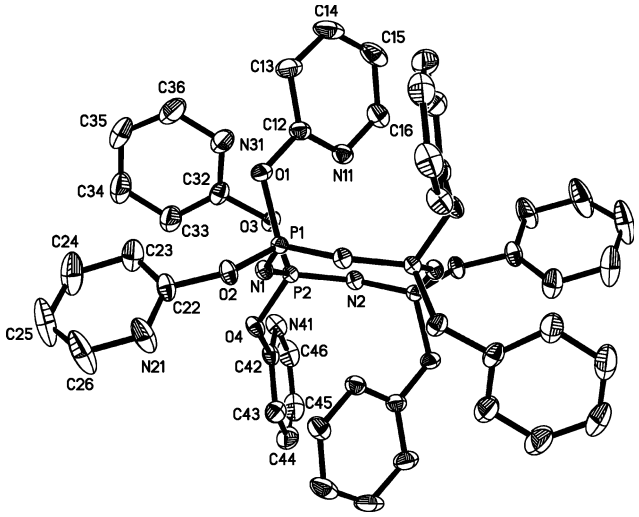

Fig. 1. ORTEP diagram of $N_4P_4(OC_5H_4N)_8$ (**1**) (ellipsoids drawn at 50% probability level).

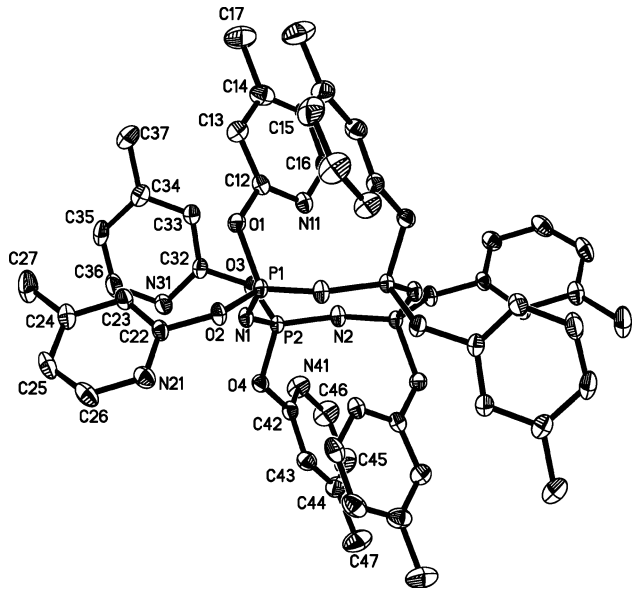

Fig. 2. ORTEP diagram of $N_4P_4(OC_6H_6N)_8{\cdot}2CH_2Cl_2$ (**2**) (ellipsoids drawn at 50% probability level).

of octachlorocyclotetraphosphazene [8], which is commonly used as a starting material for functionalised cyclotetraphosphazenes but the boat conformation is more common for aryloxy-cyclotetraphosphazenes, e.g. $N_4P_4(OC_6H_5)_8$ [9]. Ab initio molecular orbital calculations [10] on cyclophosphazene rings show the ring skeleton to be highly polar with a build up of charge density on the nitrogen atoms and nodes at the phosphorus atoms. This is in line with the experimental observation that the more positive phosphorus atoms are the preferred sites for nucleophilic attack [11]. Hence the stability of the chair conformation of the pyridyloxy-derivatives **1** and **2** can be explained by the attraction of the pyridyl-nitrogens [N(11) and N(11#)] towards the

phosphazene ring, in particular the phosphorus atoms, P(2) and P(2#). The pyridyl rings can, therefore, be envisaged to be adopting a 1,5-*N* plug arrangement, with the nitrogen atoms sitting approximately centrally on either side of the phosphazene N(1)–P(2)–N(2)···N(1#)–N(2#)–P(2#) plane, thus forcing the P(1) and P(1#) phosphorus atoms into the observed chair position (Scheme 1). The distance of the pyridyl-nitrogens from the least-squares plane through all phosphazene ring atoms is 2.520 Å for **1** and 2.516 Å for **2**. The average pyridyl–N···phosphazene–P distance (excluding the out of plane phosphorus atoms) being 3.268 Å which is shorter than the sum of the van der Waals radii of P and N (3.35 Å).

The geometry of the phosphazene ring in compound **3** is different from that observed for the same ring in **2** as a result of strong hydrogen bond interactions between the occluded water molecules and the octakis(4-methyl-2-pyridyloxy)cyclotetraphosphazenes (for details see Section 2.2.2). The phosphazene ring can be described as twisted, with P(1), N(1), P(2) and N(2) lying approximately in one plane and P(3), N(3), P(4) and N(4) in another (Fig. 3). These planes form an angle of 13.6° with each other. Using the same convention as above this can be described as a 1,3-N plug arrangement, with the plug nitrogens [N(11) and N(41)] coming from vicinal pyridyl groups (Scheme 1). The distance of the plugs to the least-squares plane formed by P(1) to N(4) is 2.657 and 2.939 Å, considerably larger than the distances in **1** and **2**. Accordingly, the average pyridyl–N···phosphazene–P distances (P1 and P3) are also longer, being 3.513 Å [for N(11)] and 4.121 Å [for N(41)].

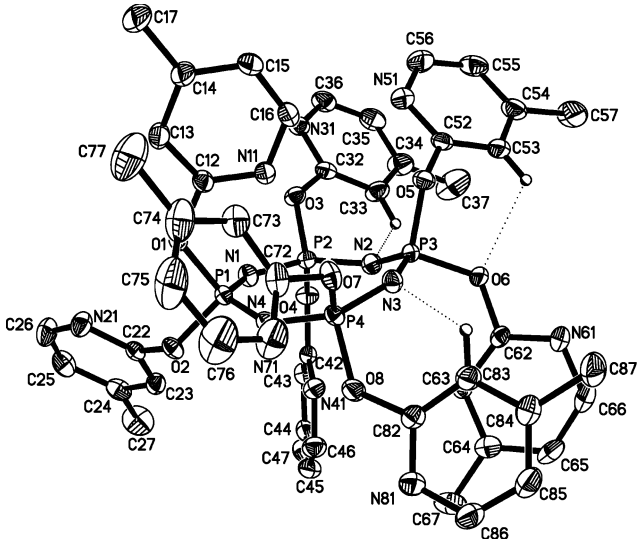

Fig. 3. ORTEP diagram of $N_4P_4(OC_6H_6N)_8 \cdot H_2O$ (**3**) (ellipsoids drawn at 50% probability level).

Selected bond lengths and angles for compounds **1**, **2** and **3** are given in Tables 1–3. For all three compounds, the P–N–P angles of the cyclotetraphosphazene rings [134.09(9)–146.0(1)°] and the endocyclic bond angles at the phosphorus atoms [122.55(9)°–125.43(6)°] are in agreement with results reported for aryloxy–cyclotetraphosphazene systems as are the average P–N bond lengths [1.559 Å for **1**, 1.554 Å for **2** and 1.559 Å for **3**] [9,12]. Compared with $P_4N_4(OC_6H_5)_8$ [9], the pyridyloxy-cyclotetraphosphazenes exhibit larger average P–O

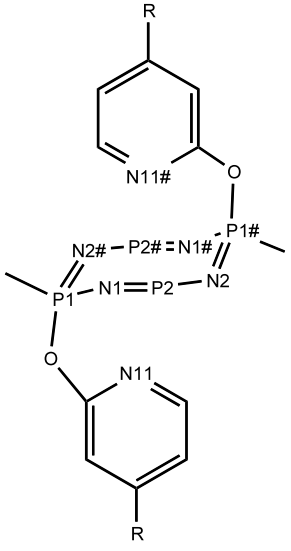

chair 1,5-*N* plug arrangement in **1** R = H) and **2** (R = CH_3)

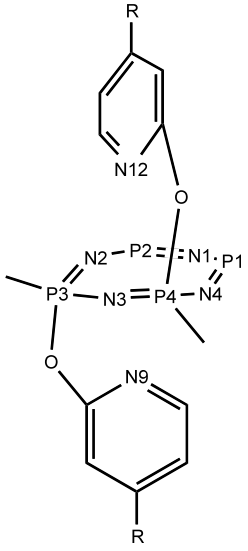

twisted 1,3-*N* plug arrangement in 3 (R = CH_3)

Scheme 1. *N*-plug arrangements in **1**, **2** and **3**. Substituents are partly omitted for clarity.

Table 1
Selected bond lengths (Å) and angles (°) for $N_4P_4(OC_5H_4N)_8$ (**1**)

Bond lengths	
P(1)–N(1)	1.5542(11)
P(1)–N(2)#1	1.5615(11)
P(1)–O(2)	1.5935(9)
P(1)–O(1)	1.6203(9)
N(1)–P(2)	1.5613(11)
P(2)–N(2)	1.5606(11)
P(2)–O(3)	1.5967(9)
P(2)–O(4)	1.6043(10)
Bond angles	
N(1)–P(1)–N(2)#1	123.52(6)
N(2)–P(2)–N(1)	125.43(6)
P(1)–N(1)–P(2)	141.08(8)
P(2)–N(2)–P(1)#1	138.66(8)
O(2)–P(1)–O(1)	97.96(5)
O(3)–P(2)–O(4)	105.20(5)

Symmetry transformations used to generate equivalent atoms: #1 $-x+2, -y, -z$.

Table 2
Selected bond lengths (Å) and angles (°) for $N_4P_4(OC_6H_6N)_8 \cdot 2CH_2Cl_2$ (**2**)

Bond lenghts	
P(1)–N(2)#1	1.5422(14)
N(1)–P(1)	1.5572(14)
P(1)–O(1)	1.6272(12)
P(1)–O(2)	1.5852(12)
P(2)–N(1)	1.5661(14)
N(2)–P(2)	1.5511(14)
P(2)–O(3)	1.5946(12)
P(2)–O(4)	1.5997(12)
Bond angles	
N(2)#1–P(1)–N(1)	123.26(8)
N(2)–P(2)–N(1)	124.65(8)
P(1)–N(1)–P(2)	134.09(9)
P(1)#1–N(2)–P(2)	146.01(10)
O(2)–P(1)–O(1)	98.05(6)
O(3)–P(2)–O(4)	105.91(7)

Symmetry transformations used to generate equivalent atoms: #1 $-x+2, -y, -z+2$

distances [1.604 Å in **1**, 1.602 Å in **2** and **3** cf. 1.582 Å] but the average exocyclic O–P–O angles are similar [101.58° for **1**, 101.98° for **2** and 100.66° for **3** cf. 102.3°].

The orientation of the pyridyl rings in compounds **1** and **2** is very similar. With respect to the plug-pyridyl rings, it is observed the other pyridyl rings are in a staggered arrangement above and below the phosphazene plane with each ring angled, pointing an appropriate hydrogen to the π-cloud of its *trans-vicinal* neighbour. In contrast, compound **3** contains two domains of parallel and antiparallel[1] (with respect to the 4-methyl group) stacked pyridyl rings, with intra- and intermolecular van der Waals interfaces. The orientation of two of the pyridyl rings with respect to the cyclotetraphosphazene ring allows the formation of intramolecular hydrogen bonds between hydrogen atoms on their *ortho*-carbons [H(83) and H(33)] and phosphazene ring nitrogens (Fig. 3, Table 6). There is also an intramolecular hydrogen bond between H(53) and the phenolate oxygen O(6) on the *geminal*-pyridyl ring.

[1] The parallel rings are those containing the pyridyl nitrogen atoms, N(31) and N(51) and the antiparallel rings, N(61) and N(81).

Table 3
Selected bond lengths (Å) and angles (°) for $N_4P_4(OC_6H_6N)_8 \cdot H_2O$ (**3**)

Bond lenghts	
P(1)–N(1)	1.5589(16)
P(1)–N(4)	1.5635(16)
P(1)–O(2)	1.5895(13)
P(1)–O(1)	1.6132(13)
N(1)–P(2)	1.5547(16)
P(2)–N(2)	1.5647(16)
P(2)–O(3)	1.5983(13)
P(2)–O(4)	1.6103(13)
N(2)–P(3)	1.5611(16)
P(3)–N(3)	1.5515(16)
P(3)–O(5)	1.5987(13)
P(3)–O(6)	1.6063(13)
N(3)–P(4)	1.5601(16)
P(4)–N(4)	1.5533(16)
P(4)–O(7)	1.5980(14)
P(4)–O(8)	1.6019(14)
Bond angles	
N(1)–P(1)–N(4)	123.60(9)
N(1)–P(2)–N(2)	123.68(9)
N(3)–P(3)–N(2)	122.55(9)
N(4)–P(4)–N(3)	123.84(9)
P(2)–N(1)–P(1)	141.09(11)
P(3)–N(2)–P(2)	141.98(11)
P(3)–N(3)–P(4)	141.72(11)
P(4)–N(4)–P(1)	143.81(11)
O(2)–P(1)–O(1)	98.90(7)
O(3)–P(2)–O(4)	97.76(7)
O(5)–P(3)–O(6)	100.32(7)
O(7)–P(4)–O(8)	105.64(8)

2.2.2. Tunnel formation within the crystal lattices

The main difference in the crystal packing of the 2-pyridyloxy-cyclotetraphosphazenes, **1**, **2** and **3**, when compared with the aryloxy-cyclotetraphosphazenes,

Table 4
Hydrogen bonds for $N_4P_4(OC_5H_4N)_8$ (**1**) [Å and °]

D–H···A	*d*(D–H)	*d*(H···A)	*d*(D···A)	<(DHA)
C(14)–H(14)···N(2)#2	0.95	2.53	3.3923(19)	151.6
C(45)–H(45)···O(2)#3	0.95	2.56	3.3941(18)	146.5
C(15)–H(15)···N(41)#2	0.95	2.58	3.494(2)	161.9
C(44)–H(44)···N(31)#4	0.95	2.67	3.380(2)	131.7

Symmetry transformations used to generate equivalent atoms: #1 $-x+2, -y, -z$; #2 $-x+5/2, y-1/2, -z+1/2$; #3 $x, y+1, z$; #4 $x-1/2, -y+1/2, z-1/2$.

Table 5
Hydrogen bonds for $N_4P_4(OC_6H_6N)_8 \cdot 2CH_2Cl_2$ (**2**) [Å and °]

D–H···A	d(D–H)	d(H···A)	d(D···A)	<(DHA)
C(45)–H(45)···O(1)#2	0.95	2.54	3.450(2)	160.4
C(17)–H(17B)···N(41)#3	0.98	2.56	3.509(3)	164.4
C(26)–H(26)···N(31)#4	0.95	2.62	3.565(2)	174.8
C(37)–H(37B)···O(2)#5	0.98	2.63	3.576(2)	163.2

Symmetry transformations used to generate equivalent atoms: #1 $-x+2, -y, -z+2$; #2 $x, y, z+1$; #3 $-x+1, -y, -z+2$; #4 $-x+2, -y+1, -z+2$; #5 $x-1, y, z$.

arises from the involvement of the pyridine ring nitrogen atoms in hydrogen bonded networks (see Tables 4–6). The phosphazene rings of compounds **1** and **2** lie on the corners of their unit cells (Figs. 4 and 5) but in **2** the centre of the cell is occupied by two dichloromethane molecules per cyclophosphazene whereas in **1** it contains another octakis(2-pyridyloxy)cyclotetraphosphazene molecule. In contrast, compound **3** crystallises in a considerably larger unit cell [10,087.3(2) $Å^3$ cf 1,407.23(8) and 2,093.21(5) $Å^3$] with the phosphazene rings in a quasi-hexagonal closest packing arrangement, each phosphazene molecule being surrounded by 12 others (Fig. 6). The resulting channels are occupied by water molecules.

The packing diagrams show that the different structures arise from the formation of a variety of intermolecular hydrogen bond contacts. For **2** (Fig. 5 and Table 5) these are between the phenolate oxygen of one pyridyloxy substituent and a hydrogen of the pyridine ring of another [C(45)–H(45)···O(1)#2: 2.54 Å, 160.4°], a phenolate oxygen and a methyl hydrogen [C(37)–H(37)···O(2)#5: 2.63 Å, 163.2°], a pyridine nitrogen and a pyridine ring hydrogen [C(26)–H(26)···N(31)#4: 2.62 Å, 174.8°] and another pyridine nitrogen with a methyl hydrogen [C(17)–H(17B)···N(41)#3: 2.56 Å, 164.4°]. The result is the phosphazene molecules form hollow hydrophobic tunnels through the lattice along the *a* axis with the dichloromethane molecules enclosed. The diameter of these tunnels is approximately 7.5 Å with the incorporated dichloromethane molecules being regularly spaced nearly 6 Å apart (C···C distance: 5.962 and 6.336 Å). The weak interaction of the solvent-guest with the host lattice is consistent with the behaviour of **2** when exposed to air—the transparent cubic crystals loose solvent quickly, becoming opaque. It is somewhat surprising that the dichloromethane molecules are crystallographically well defined since the shortest distances between the atoms of the CH_2Cl_2 and phosphazene molecules are all greater than the sum of the appropriate van der Waals radii[2]. For instance, the nearest hydrogen contacts to the pyridyl nitrogen atoms are at 2.819 Å [H(1A)···N(41)], 2.832 Å [H(1A)···N(31)] and 3.159 Å [H(1B)···N(21)]. The closest atoms of the phosphazene to the CH_2Cl_2 chlorines are H(15) [Cl(1)···H(15): 3.061 Å] H(47A) [Cl(1)···H(47A): 3.153 Å], H(27B) [Cl(2)···H(27B): 3.107 Å] and N(41) [Cl(2)···N(41): 3.668 Å].

Table 6
Hydrogen bonds for $N_4P_4(OC_6H_6N)_8 \cdot H_2O$ (**3**) [Å and °]

D–H···A	d(D–H)	d(H···A)	d(D···A)	<(DHA)
O(9)–H(1)···N(61)#1	1.00(4)	1.98(4)	2.945(3)	161(3)
O(9)–H(2)···N(81)#2	1.03(6)	2.16(6)	3.077(3)	147(4)
C(13)–H(13)···N(31)#3	0.95	2.42	3.373(3)	175.6
C(53)–H(53)···O(6)	0.95	2.46	3.016(2)	117.0
C(36)–H(36)···N(21)#4	0.95	2.51	3.387(3)	154.0
C(83)–H(83)···N(3)	0.95	2.55	3.116(3)	118.7
C(47)–H(47B)···O(8)#5	0.98	2.58	3.481(3)	152.1
C(27)–H(27A)···O(2)#5	0.98	2.58	3.208(3)	122.0
C(33)–H(33)···N(2)	0.95	2.61	3.224(3)	123.0
C(17)–H(17A)···O(4)#3	0.98	2.61	3.419(3)	140.5

Symmetry transformations used to generate equivalent atoms: #1 $x+1/2, -y+3/2, -z+1$; #2 $x, y, z+1$; #3 $-x+1, y+1/2, -z+1/2$; #4 $-x+1, y-1/2, -z+1/2$; #5 $-x+3/2, y-1/2, z$.

In compound **3**, the more strongly interacting guest water molecules (c.f. CH_2Cl_2 in **2**) causes the diameter of the phosphazene host's tunnels to contract considerably by about 2 Å to approximately 5.5 Å. The hydrogen atoms, H(1) and H(2), of the H_2O molecules in the lattice of **3** form strong hydrogen bonds to the pyridyl nitrogens N(61) [O(9)–H(1)···N(61): 1.98(4) Å, 161(3)°] and N(81) [O(9)–H(2)···N(81): 2.16(5) Å, 147(4)°]. Concomitantly, the orientation of the pyridyl rings changes. The planes of the pyridyl rings in **2** are approximately aligned parallel to the tunnels, effectively lining it with a nonpolar wall, whereas in **3,** the rings are almost perpendicular to the walls which causes their equatorial hydrogens to penetrate into the tunnel. The phosphazene entities are interconnected by a hydrogen bond network between pyridyl nitrogens and pyridyl ring hydrogens [C(13)–H(13)···N(31)#3: 2.42 Å, 175.6° and C(36)–H(36)···N(21)#4: 2.51 Å, 154.0°] and between phenolate oxygens and methyl hydrogens [C(27)–H(27A)···O(2)#5: 2.58 Å, 122.0° and C(17)–H(17A)···O(4)#3: 2.61 Å, 140.5°]. Along the tunnels the van der Waals interfaces of the antiparallel pyridyl rings (described in Section 2.2.1) i.e. the rings containing atoms N(61) to C(67) and N(81) to C(87)] give a stacked arrangement of the aromatic rings at 3.4 Å (intermolecular) and 3.6 Å (intramolecular) distances.

In contrast to the host–guest structures observed for **2** and **3**, in compound **1** (Fig. 4) does not have occluded guest molecules in its lattice. Instead a phosphazene ring nitrogen shows intermolecular hydrogen contacts with a pyridine ring hydrogen [C(14)–H(14)···N(2)#2: 2.53 Å, 151.6°] as well as between a pyridine nitrogen atom and an aromatic ring hydrogen [C(15)–H15)···N(41)#2: 2.58 Å, 161.9°] and a pyridyloxy oxygen with a another

[2] 2.75 Å for N and H, 2.95 Å for Cl and H, 3.30 Å for N and Cl.

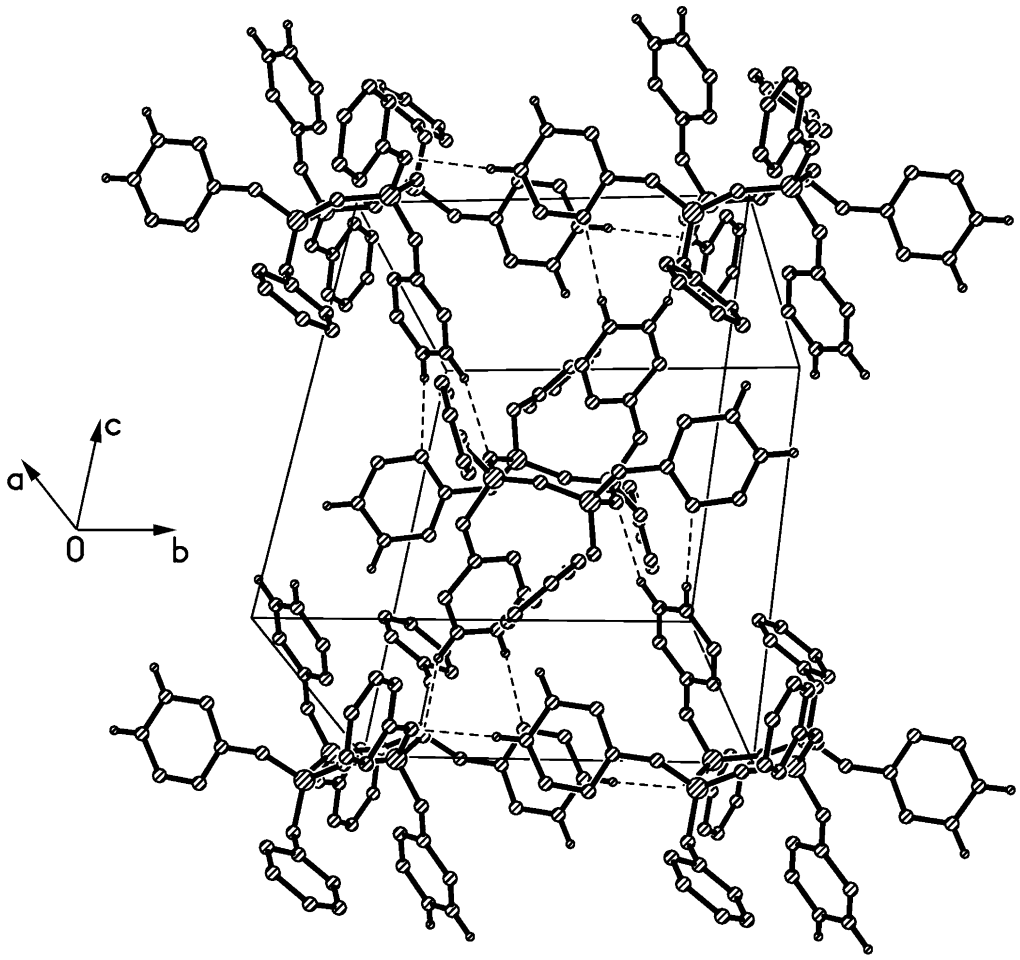

Fig. 4. Packing diagram of **1** showing one hydrogen-bonded sheet along the $(10\bar{1})$ layer.

ring hydrogen [C(45)–H(45)···O(2)#3: 2.56 Å, 146.5°]. These contacts result in the formation of cyclophosphazene entities along the $(10\bar{1})$ layer that are interconnected via van der Waals interactions between parallel pyridyl rings of adjacent molecules. The ability of **1** to accommodate another cyclophosphazene moiety within its unit cell may be linked to the involvement of its phosphazene ring nitrogen in the hydrogen-bond network. In contrast, the introduction of the 4-methyl group into the pyridyloxy substituent in **2** and **3** gives rise to different hydrogen contacts, resulting in the formation of tunnels along one crystallographic axis. It is remarkable that these tunnels persist, even when the subtle network is disturbed by incorporation of strongly interacting guest water molecule.

In contrast to the results reported in this paper for the pyridyloxy-substituted cyclotetraphosphazenes, another study [13] shows that a host framework, derived from the acceptor–donor complex formed from guanidinium (G) and 4,4′-biphenyldisulfonate (BPDS), gives rise to clathrates with a range of aromatic guests with the composition (G)(2BPDS)·(guest). On going from toluene to halogenated-benzene guests, the sizes of the pores in the host decrease suggesting attractive host–guest interactions between the halogen atoms and the guanidinium sulfonate sheets. However, with 1,4-dibromobenzene as guest, the host crystallises in a different structure with larger pores due to pronounced steric effects.

How strong the tendency for tunnel formation is in pyridyloxy-substituted cyclotetraphosphazenes and whether this can be further fine-tuned by functionalisation of the pyridyloxy-groups needs further investigation. A greater understanding of the factors that cause channels to form in the lattices of cyclotetraphosphazenes has the potential to yield crystal-hosts that can be tuned to meet the specific demands of the guest molecule.

3. Experimental

3.1. General

All synthetic steps were carried out under nitrogen using standard Schlenk techniques. Analytical grade

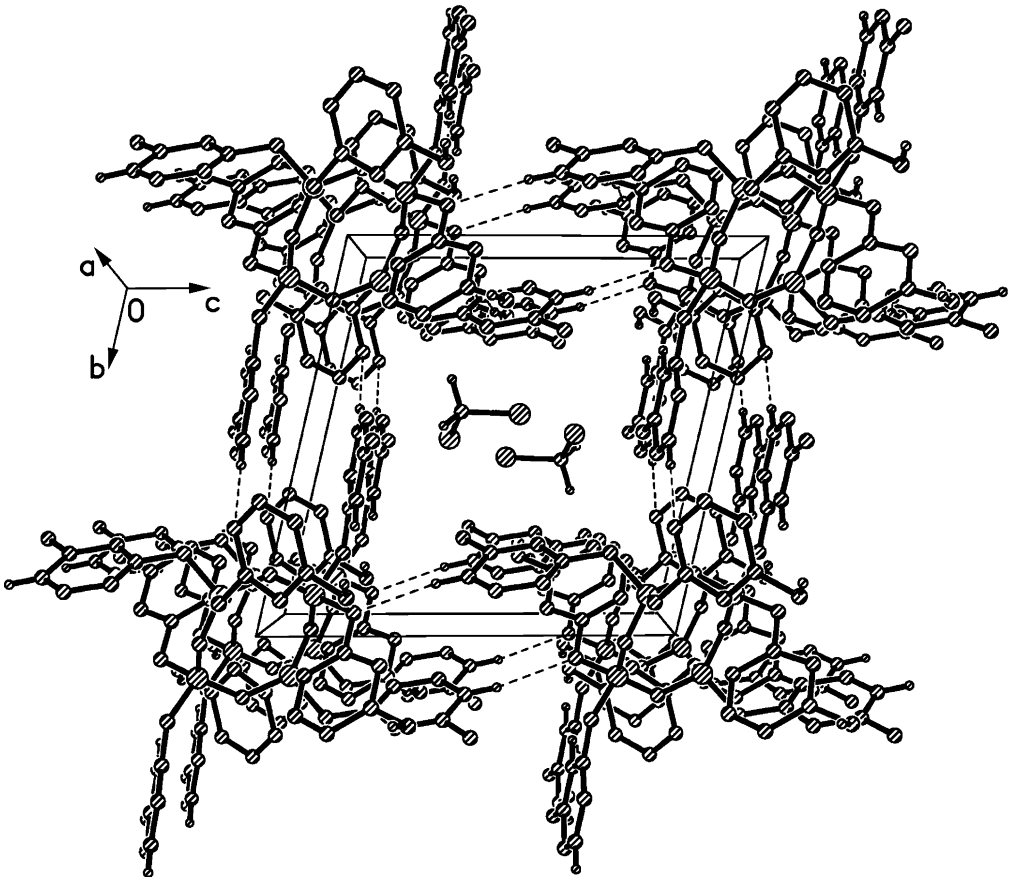

Fig. 5. Packing diagram of **2** viewed down the *a* axis.

solvents were purchased from standard chemical suppliers, and with the exception of tetrahydrofuran (THF), were used without further purification or drying. The THF was distilled from sodium wire/benzophenone and stored over activated molecular sieve (4 Å). 2-Hydroxypyridine (Lancaster) and 2-hydroxy-4-methylpyridine (Aldrich) were used as received. NaH (Riedel-de-Haën) was isolated as a pure powder from a paraffin oil mixture by washing with hexane. NMR spectra were recorded on a Bruker Avance 400 spectrometer, operating at 400 MHz. Electrospray mass spectra were collected from CH_3CN solutions on a micromass ZMD spectrometer, run in positive ion mode.

3.2. Synthesis of compounds

Compounds **1** and **2** were synthesised from the reaction of $N_4P_4Cl_8$ and 2-hydroxypyridine or 4-methyl-2-hydroxypyridine, respectively, under reflux in THF using NaH as base following the method described for $N_3P_3(OC_6F_5)_6$ [14]. The reactions were monitored using ^{31}P NMR.

Yields (%): 47 (**1**), 58 (**2**).

Characterisation data for compound **1:** m.p. 153–155 °C; ^{31}P NMR ($CDCl_3$): δ −17.5 (s. 4P); ESMS *m*/*z* 933 (MH^+); *Anal*. Calc. for $C_{40}H_{32}N_{12}O_8P_4$: C, 51.51; H, 3.46; N, 18.02. Found: C, 51.74; H, 3.34; N, 18.12%.

Characterisation data for compound **2:** Since **2** readily loses the lattice CH_2Cl_2, data are for the unsolvated compound: m.p. 95–104 °C; ^{31}P NMR ($CDCl_3$): δ −17.9 (s. 4P); ESMS *m*/*z* 1045 (MH^+); *Anal*. Calc. for $C_{48}H_{48}N_{12}O_8P_4$: C, 55.18; H, 4.63; N, 16.09. Found: C, 55.11; H, 4.61; N, 16.31%.

3.3. Crystal structure determination of compound *1*

Single crystals of $N_4P_4(OC_5H_4N)_8$ were recrystallised via slow CH_2Cl_2-pentane diffusion, mounted in inert oil (Paratone N, Exxon) and transferred into the cold gas stream of a Siemens SMART CCD area-detector diffractometer. Crystal data for $C_{40}H_{32}N_{12}O_8P_4$: M = 932.66, monoclinic, space group $P2_1/n$, $a = 11.7784(2)$, $b = 11.84850(10)$, $c = 15.7113(2)$ Å, $\beta = 107.32°$, $V = 2093.21(5)$ Å^3, $T = 150(2)$ K, $Z = 2$, $D_{calc} = 1.480$ g cm^{-3}, $F = 960$, μ(Mo Kα) = 1.45 mm^{-1}, 12 093 reflections were collected ($3.82° < 2\theta < 52.77°$), of which 4264 were unique ($R_{int} = 0.0146$). Data were corrected for absorption effects (SADABS); $T_{max} = 0.9610$, $T_{min} = 0.8858$. Refinement of 289 parameters converged at $R_1 = 0.0303$ [observed data: 3837 $|F_o| > 4\sigma(F_o)$], $wR_2(F^2) = 0.0858$ (all data).

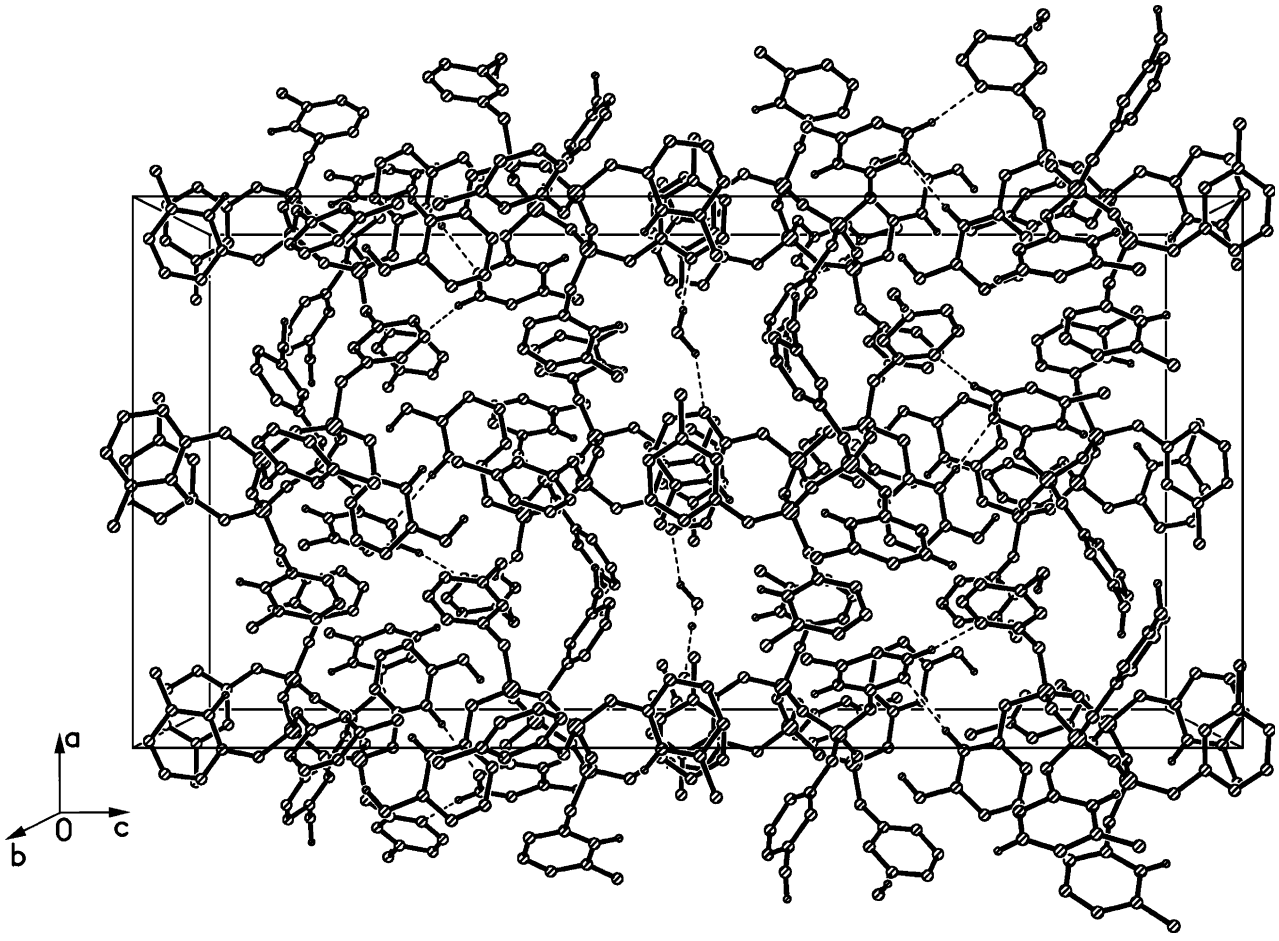

Fig. 6. Packing diagram of **3** viewed down the *b* axis.

3.4. Crystal structure determination of compound **2**

Single crystals of $N_4P_4(OC_6H_6N)_8\cdot 2CH_2Cl_2$ were recrystallised via slow CH_2Cl_2-pentane diffusion, mounted in inert oil (Paratone N, Exxon) and transferred into the cold gas stream of a Siemens SMART CCD area-detector diffractometer. Crystal data for $C_{50}H_{52}Cl_4N_{12}O_8P_4$: $M = 1214.72$, triclinic, space group $P\bar{1}$, $a = 10.3201(3)$, $b = 11.7008(4)$, $c = 11.9878(4)$ Å, $\alpha = 102.874(1)^\circ$, $\beta = 93.133(1)^\circ$, $\gamma = 92.151(1)^\circ$, $V = 1407.23(8)$ Å^3, $T = 150(2)$ K, $Z = 1$, $D_{calc} = 1.433$ g cm^{-3}, $F = 628$, μ(Mo Kα) = 1.45 mm^{-1}, 11552 reflections were collected ($3.50^\circ < 2\theta < 52.87^\circ$), of which 5694 were unique ($R_{int} = 0.0135$). Data were corrected for absorption effects (SADABS); $T_{max} = 0.9627$, $T_{min} = 0.8613$. Refinement of 356 parameters converged at $R_1 = 0.0362$ [observed data: 5011 $|F_o| > 4\sigma(F_o)$], $wR_2(F^2) = 0.0976$ (all data).

3.5. Crystal structure determination of compound **3**

Single crystals of $N_4P_4(OC_6H_6N)_8\cdot H_2O$ were recrystallised via slow evaporation of a dichloropropane solution, mounted in inert oil (Paratone N, Exxon) and transferred into the cold gas stream of a Siemens SMART CCD area-detector diffractometer. Crystal data for $C_{48}H_{50}N_{12}O_9P_4$: $M = 1062.88$, orthorhombic, space group *Pbca*, $a = 18.6149(2)$, $b = 14.4657(2)$, $c = 37.4605(3)$ Å, $V = 10087.27(19)$ Å^3, $T = 150(2)$ K, $Z = 8$, $D_{calc} = 1.400$ g cm^{-3}, $F = 4432$, μ(Mo Kα) = 1.45 mm^{-1}, 57 240 reflections were collected ($2.18^\circ < 2\theta < 52.23^\circ$), of which 9885 were unique ($R_{int} = 0.0228$). Data were corrected for absorption effects (SADABS); $T_{max} = 0.9710$, $T_{min} = 0.8738$. Refinement of 674 parameters converged at $R_1 = 0.0387$ [observed data: 8639 $|F_o| > 4\sigma(F_o)$], $wR_2(F^2) = 0.0977$ (all data).

4. Supplementary material

Crystallographic data for the structural analysis has been deposited with the Cambridge Crystallographic Data Centre, CCDC Nos. 189721 (**1**), 189722 (**2**) and 189723 (**3**). Copies of this information may be obtained free of charge from: The Director, CCDC, 12 Union Road, Cambridge, CB2 1EZ, UK (fax: +44-1223-336033; e-mail: deposit@ccdc.cam.ac.uk or www: http://www.ccdc.cam.ac.uk).

Acknowledgements

We gratefully acknowledge the financial support and the award of a postdoctoral fellowship (to A.D.) from the Massey University Research Fund. We thank Associate Professor C.E.F. Rickard (University of Auckland) for collection of X-ray data and Professor G.B. Jameson for useful discussions. The skilled technical help of H.R. Payne and G.H. Freeman is also acknowledged.

References

[1] G.R. Desiraju, Nature 412 (2001) 397.
[2] (a) V.A. Russell, C.C. Evans, W. Li, M.D. Ward, Science 276 (1997) 575;
(b) C.C. Evans, L. Sukarto, M.D. Ward, J. Am. Chem. Soc. 121 (1999) 320;
(c) J.-M. Lehn, Chem. Eur. J. 3 (1997) 99;
(d) A.A. Khan, S.T. Bramwell, K.D.M. Harris, B.M. Kariuki, M.R. Truter, Chem. Phys. Lett. 307 (1999) 320;
(e) S. Noro, S. Kitagawa, M. Kondo, K. Seki, Angew. Chem., Int. Ed. Engl. 39 (2000) 2081.
[3] G.R. Desiraju, T. Steiner, The Weak Hydrogen Bond in Structural Chemistry and Biology, Oxford University Press, Oxford, 1999.
[4] H.R. Allcock, A.P. Primrose, E.N. Silverberg, K.B. Visscher, A.L. Rheingold, I.A. Guzei, M. Parvez, Chem. Mater. 12 (2000) 2530 (and references therein).
[5] (a) K. Kubono, N. Asaka, T. Taga, S. Isoda, T. Kobayashi, J. Mater. Chem. 4 (1994) 291;
(b) K. Kubono, N. Asaka, S. Isoda, T. Kobayashi, T. Taga, Acta Crystallogr., Sect. C 50 (1994) 324;
(c) A. Comotti, R. Simonutti, S. Stramare, P. Sozzani, Nanotechnology 10 (1999) 70;
(d) A. Comotti, M.C. Gallazzi, R. Simonutti, P. Sozzani, Chem. Mater. 10 (1998) 3589.
[6] H.R. Allcock, N.J. Sunderland, Macromolecules 34 (2001) 3069 (and references therein).
[7] V. Chandrasekhar, K.R. Justin Thomas, Structure Bonding 81 (1993) 41.
[8] A.J. Wagner, A. Vos, Acta Crystallogr., Sect. B 24 (1968) 707.
[9] H.R. Allcock, A.A. Dembek, M.N. Mang, G.H. Riding, M. Parvez, K.B. Visscher, Inorg. Chem. 31 (1992) 2734.
[10] (a) R. Jaeger, M. Debowski, I. Manners, G.J. Vancso, Inorg. Chem. 38 (1999) 1153;
(b) V. Luaña, A.M. Pendás, A. Costales, G.A. Carriedo, F.J. García-Alonso, J. Phys. Chem. A 105 (2001) 5280.
[11] C.W. Allen, Coord. Chem. Rev. 130 (1994) 137.
[12] (a) G.B. Ansell, G.J. Bullen, J. Chem. Soc. A (1971) 2498.;
(b) H.R. Allcock, D.C. Ngo, M. Parvez, R.R. Whittle, W.J. Birdsall, J. Am. Chem. Soc. 113 (1991) 2628;
(c) H.R. Allcock, S. Al-Shali, D.C. Ngo, K.B. Visscher, M. Parvez, J. Chem. Soc., Dalton Trans. (1995) 3521.;
(d) H.R. Allcock, S. Al-Shali, D.C. Ngo, K.B. Visscher, M. Parvez, J. Chem. Soc., Dalton Trans. (1996) 2393.;
(e) H.R. Allcock, S. Al-Shali, D.C. Ngo, K.B. Visscher, M. Parvez, J. Chem. Soc., Dalton Trans. (1996) 3549.
[13] J.A. Swift, A.M. Reynolds, M.D. Ward, Chem. Mater. 10 (1998) 4159.
[14] C.V. Depree, E.W. Ainscough, A.M. Brodie, A.K. Burrell, C. Lensink, B.K. Nicholson, Polyhedron 19 (2000) 2101.